

## Three-dimensional nonlinear prediction of tooth movement from the force system and root morphology

Roberto Savignano<sup>a</sup>; Rodrigo F. Viecilli<sup>b</sup>; Udochukwu Oyoyo<sup>c</sup>

### ABSTRACT

**Objectives:** To determine the different impact of moment-to-force ratio (M:F) variation for each tooth and spatial plane and to develop a mathematical model to predict the orthodontic movement for every tooth.

**Materials and Methods:** Two full sets of teeth were obtained combining cone-beam computed tomography (CBCT) and optical scans for two patients. Subsequently, a finite element analysis was performed for 510 different force systems for each tooth to evaluate the centers of rotation.

**Results:** The center of  $C_{ROT}$  locations were analyzed, showing that the M:F effect was related to the spatial plane on which the moment was applied, to the force direction, and to the tooth morphology. The tooth dimensions on each plane were mathematically used to derive their influence on the tooth movement.

**Conclusion:** This study established the basis for an orthodontist to determine how the teeth move and their axes of resistance, depending on their morphology alone. The movement is controlled by a parameter ( $k$ ), which depends on tooth dimensions and force system features. The  $k$  for a tooth can be calculated using a CBCT and a specific set of covariates. (*Angle Orthod.* 2020;90:811–822.)

**KEY WORDS:** Tooth movement; Biomechanics; Finite element analysis; Orthodontics

### INTRODUCTION

The load system delivered by an orthodontic appliance to a specific tooth is the most important determinant factor in the quality of the resulting orthodontic movement. The resulting tooth movement in three dimensions (3D) will depend on specific 3D moment-to-force ratio (M:F) combinations. The current method to describe the type of tooth movement consists of measuring the distance from the tooth's projected axis of rotation (center of rotation;  $C_{ROT}$ ) to the virtual intersection of the axes of resistance (center of resistance;  $C_{RES}$ ). Some recent studies<sup>1–4</sup> and many

previous studies<sup>5–9</sup> investigated the role of M:F associated with different tooth movements. One classic study focused on applying a force perpendicular to a canine long axis with a parabolic shaped root, obtaining the Burstone formula ( $M:F = 0.068 \times h^2/y$ ), where  $h$  is the distance from the alveolar crest to the apex and  $y$  is the distance between the  $C_{RES}$  and the  $C_{ROT}$ .<sup>5</sup>

A previous study demonstrated a nonlinear relationship between tooth movement and force system directions and that the Burstone formula must be modified depending on them. In addition, different types of nonlinear behavior depend on the applied force and moment directions. This behavior was demonstrated for an upper first premolar with average dimension.<sup>10</sup>

The hypothesis of the current article was that this phenomenon is due to root asymmetries and specific differences in tooth morphology. The purpose was to describe which tooth morphological characteristics determine this nonlinear behavior and statistically test if tooth movement in any direction can be predicted if data on root morphology and the original force system are provided to the orthodontist.

The specific objective was to determine the relationships between all meaningful permutations of M:F and

<sup>a</sup> Assistant Professor, Center for Dental Research, School of Dentistry, Loma Linda University, Loma Linda, Calif.

<sup>b</sup> Adjunct Associate Professor, Center for Dental Research, School of Dentistry, Loma Linda University, Loma Linda, Calif.

<sup>c</sup> Assistant Professor, Dental Education Services, School of Dentistry, Loma Linda University, Loma Linda, Calif.

Corresponding author: Dr Roberto Savignano, Center for Dental Research, School of Dentistry, Loma Linda University, 11175 Campus Street A1010, Loma Linda, CA 92350, USA (e-mail: rsavignano@llu.edu)

Accepted: June 2020. Submitted: December 2019.

Published Online: September 14, 2020

© 2020 by The EH Angle Education and Research Foundation, Inc.

**Table 1.** Tooth Dimensions for the Two Data Sets

	MD, mm	LB, mm	Root Length Plane YZ, mm	Root Length Plane ZX, mm	Root AVG, mm
<b>Patient 1</b>					
Maxillary central incisor	6.1	5.8	15.6	16.2	15.9
Maxillary lateral incisor	4.2	5.8	15.1	15.5	15.3
Maxillary canine	6.2	8.8	15.8	16.0	15.9
Maxillary first premolar	4.9	8.7	13.6	14.2	13.9
Maxillary second premolar	5.4	8.4	14.4	14.3	14.4
Maxillary first molar	7.2	9.0	13.1	12.8	13.0
Maxillary second molar	7.8	10.1	12.5	12.0	12.3
Mandibular central incisor	4.3	6.2	13.1	14.0	13.6
Mandibular lateral incisor	3.9	6.3	12.2	12.9	12.6
Mandibular canine	3.9	5.9	12.5	14.0	13.3
Mandibular first premolar	4.8	6.9	10.8	11.7	11.3
Mandibular second premolar	4.9	7.0	13.8	14.2	14.0
Mandibular first molar	9.2	9.5	11.8	12.0	11.9
Mandibular second molar	9.2	8.2	11.6	12.1	11.9
<b>Patient 2</b>					
Maxillary central incisor	6.9	7.4	13.7	15.8	14.7
Maxillary lateral incisor	4.8	6.4	12.0	13.6	12.8
Maxillary canine	6.2	7.4	16.0	16.4	16.2
Maxillary first premolar	5.5	8.4	12.3	13.3	12.8
Maxillary second premolar	6.1	8.9	13.2	13.8	13.5
Maxillary first molar	8.8	8.8	11.4	12.2	11.8
Maxillary second molar	9.2	10.8	13.2	12.8	13.0
Mandibular central incisor	3.8	5.6	11.4	12.1	11.8
Mandibular lateral incisor	3.5	5.5	10.6	11.5	11.1
Mandibular canine	3.5	5.3	10.9	12.1	11.5
Mandibular first premolar	4.4	6.2	9.4	10.1	9.8
Mandibular second premolar	4.3	6.3	12.0	12.3	12.2
Mandibular first molar	8.1	8.3	10.2	10.4	10.3
Mandibular second molar	8.1	7.3	10.1	10.5	10.3

the  $C_{ROT}$ , for different force directions, in each spatial plane (XY, YZ, ZX), for each tooth. Through finite element analysis (FEA), comparative maps of the effects of relevant M:F combinations on each tooth were built. Then, the statistical evaluation of the resulting maps was used to determine if tooth morphological features could be used to predict how the tooth will move with a specific force system. The significance of this result, under the limitations of the method, is that a clinician could derive the biomechanical behavior of any tooth if the force system and tooth dimensions are given, without having to resort to FEA.

To complete the tooth movement laws, the aim was to retrieve a statistically based 3D mathematical relationship between  $C_{RES}$  and tooth morphology. The  $C_{RES}$  coordinates were analyzed for the previous data set to also introduce a set of covariates to calculate the 3D  $C_{RES}$  coordinates based on the tooth dimensions.

## MATERIALS AND METHODS

The 3D models for each tooth were obtained from two patients according to the method described by Savignano et al.<sup>10</sup> The teeth dimensions are reported in Table 1. The root dimensions were measured consid-

ering the root part attached to the bone through the periodontal ligament (PDL). The Loma Linda University Institutional Review Board (IRB) committee determined that this research did not require IRB approval because data or specimens were not collected specifically for this study and private individually identifiable information were not received.

Each maxillary and mandibular model was manually sliced to obtain seven tooth-PDL-bone multibody models from each arch for the FEA. A total of 28 submodels were extracted. Bone and teeth were modeled as simplified homogenous bodies without discerning between cortical and cancellous bone and enamel, pulp and dentin, as was done also in previous studies because the data differences are insignificant.<sup>9-12</sup> A linear elastic model was used for each structure to test the movements under the assumption of low PDL strains (<7.5%),<sup>13</sup> as summarized in Table 2.

The geometries were imported in the Finite Element Software ANSYS Workbench 16 (ANSYS, Canonsburg, Penn), where all the bodies were meshed with solid elements.

The coordinate system was defined for each tooth according to the occlusal plane. The x-axis was congruent with the buccolingual tooth dimension,

**Table 2.** Material Properties Used for the Finite Element Analysis

Structure	Young Modulus, MPa	Poisson's Ratio
Tooth	20,000	0.3
Bone	2000	0.3
Periodontal ligament	0.05	0.3

whereas the *y*-axis was congruent with the mesiodistal and the *z*-axis was perpendicular to the occlusal plane (Figure 1).

To find the  $C_{RES}$ , three simulations were run for each tooth, one for each coordinate plane, applying a moment with the specific values shown in Table 3. The moment amount was different for each tooth because each tooth requires a different load<sup>14</sup> to keep the PDL strain <7.5%, allowing for a linear PDL model within this range.<sup>15</sup>

The  $C_{RES}$  coordinates were measured with the coordinate system located at the center of the cementoenamel junction (CEJ), as shown in Figure 1.

For each tooth, the different M:F tested were applied at the respective  $C_{RES}$  to provide a generalized map of tooth movements that could be transferred to any appliance (eg, brackets, aligners).

A tooth-specific constant force was applied at the  $C_{RES}$  for each tooth as reported in Table 3, while the M:F varied from -12 mm to 12 mm. As for the moment, the forces used during the simulations were also proportionally different for each tooth, so as to keep the same strain <7.5% in the PDL for ascertaining the validity of the linear model. All of the bones' nodes were assigned zero displacement to simulate a rigid body due to the transient nature of tooth displacement solely attributed to bone deformation, as reported previously.<sup>9</sup> The simulations were performed on the three spatial planes (plane XY, plane YZ, plane ZX). For each plane, 17 equivalent force systems were applied at the  $C_{RES}$  of each tooth, as shown in the example of Figure 2. Figure 3 shows a schematic of the experimental design used for each tooth.

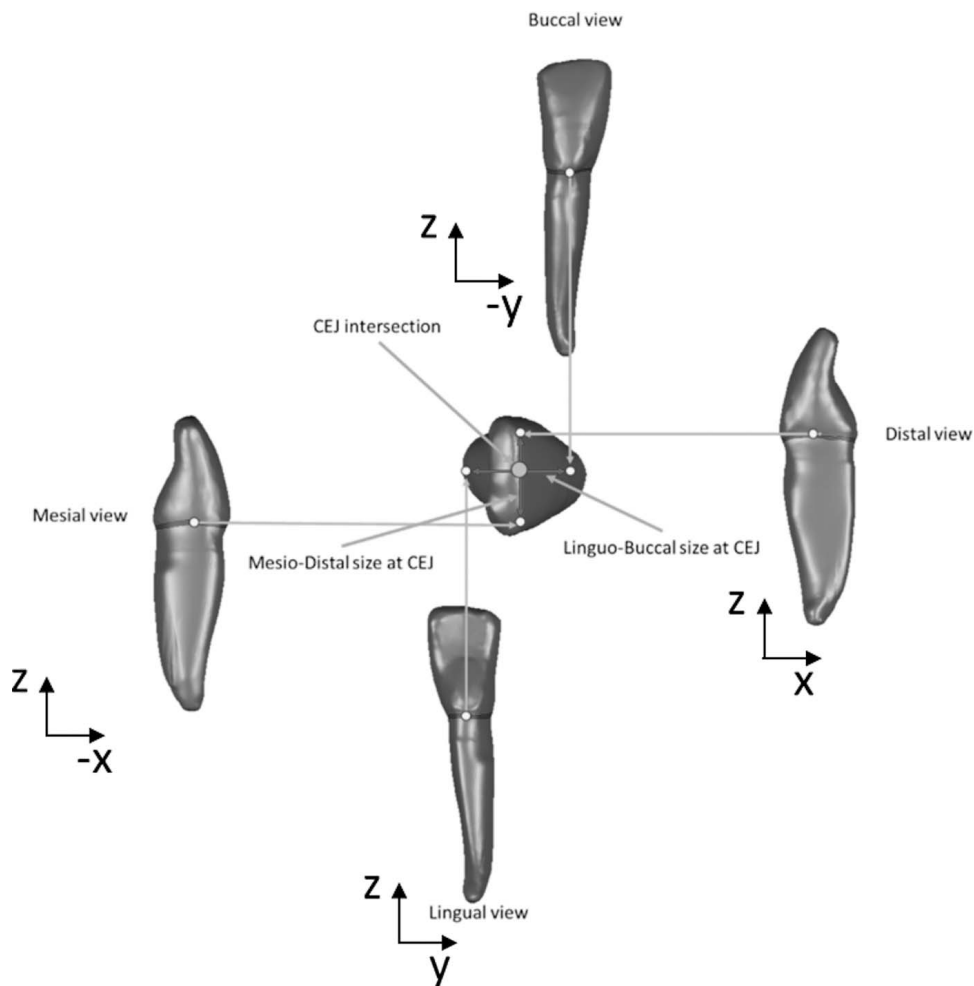


**Figure 1.** The cementoenamel junction (CEJ) intersection (yellow) used to refer the  $C_{RES}$  coordinates was defined on the plane XY as the intersection between the mesiodistal and the linguobuccal tooth dimensions. On the *z*-axis, the coordinate system was located at the average between CEJ on the mesiodistal views and CEJ on the linguobuccal views.

**Table 3.** Moment and Forces Applied to Each Tooth to Locate the Approximate Center of Resistance, Keeping the PDL Principal Strain Value Below 7.5%

	Central Incisor	Lateral Incisor	Canine	First Premolar	Second Premolar	First Molar	Second Molar
Moment, Nmm							
Maxillary	-1.8	-1.08	-1.68	-1.56	-1.56	-2.88	-3
Mandibular	-1.08	-1.08	-1.44	-1.44	-1.56	-2.76	-2.28
Force, N							
Maxillary	0.15	0.09	0.14	0.13	0.13	0.24	0.25
Mandibular	0.09	0.09	0.12	0.12	0.13	0.23	0.19

The projected axis of rotation ( $C_{ROT}$ ) was evaluated for each scenario through the displacement vectors of two nodes of the tooth.<sup>8</sup> The resulting  $C_{ROT}$  coordinates and the distances from the  $C_{RES}$  were evaluated and analyzed to obtain a mathematical relationship between M:F and  $C_{ROT}$ . The D (distance  $C_{RES} - C_{ROT}$ ) vs M:F was analyzed using CurveExpert Basic software (CurveExpert, Madison, Ala), dividing the analysis by tooth and spatial plane. The starting model was set as simple hyperbolic, as previously validated for different teeth:

$$D_{C.Res-C.Rot} = \frac{k}{MF}$$

Statistical analyses were performed with the aim of obtaining generalized formulae to locate the tooth  $C_{RES}$  and calculate an approximate k for every tooth and force system.

Multiple linear regression analysis was conducted to assess the influence of the teeth morphological data reported in Table 1 for the first data set. All hypotheses were tested at an  $\alpha = .05$  level for the second k data set. A sample size of two patients was considered appropriate for a pilot study. For statistical analysis, normality was assumed for the data even if it could not be proven because of the sample size, and the bootstrap method was applied for coefficient convergence. Multicollinearity between the independent variables was tested, discarding variables with variance inflation factor >1.5.

To evaluate the performance of the regression models, the covariates were tested on a randomly chosen tooth: a mandibular central incisor was reconstructed through a combination of cone-beam computed tomography (CBCT) and optical scanner for this purpose. The process shown in Figure 3 was

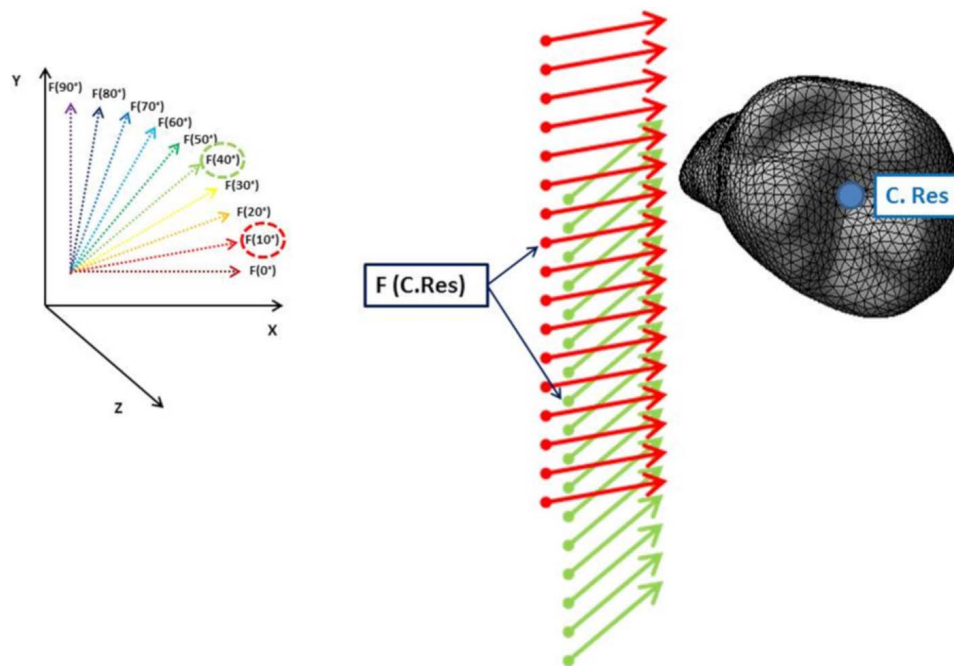
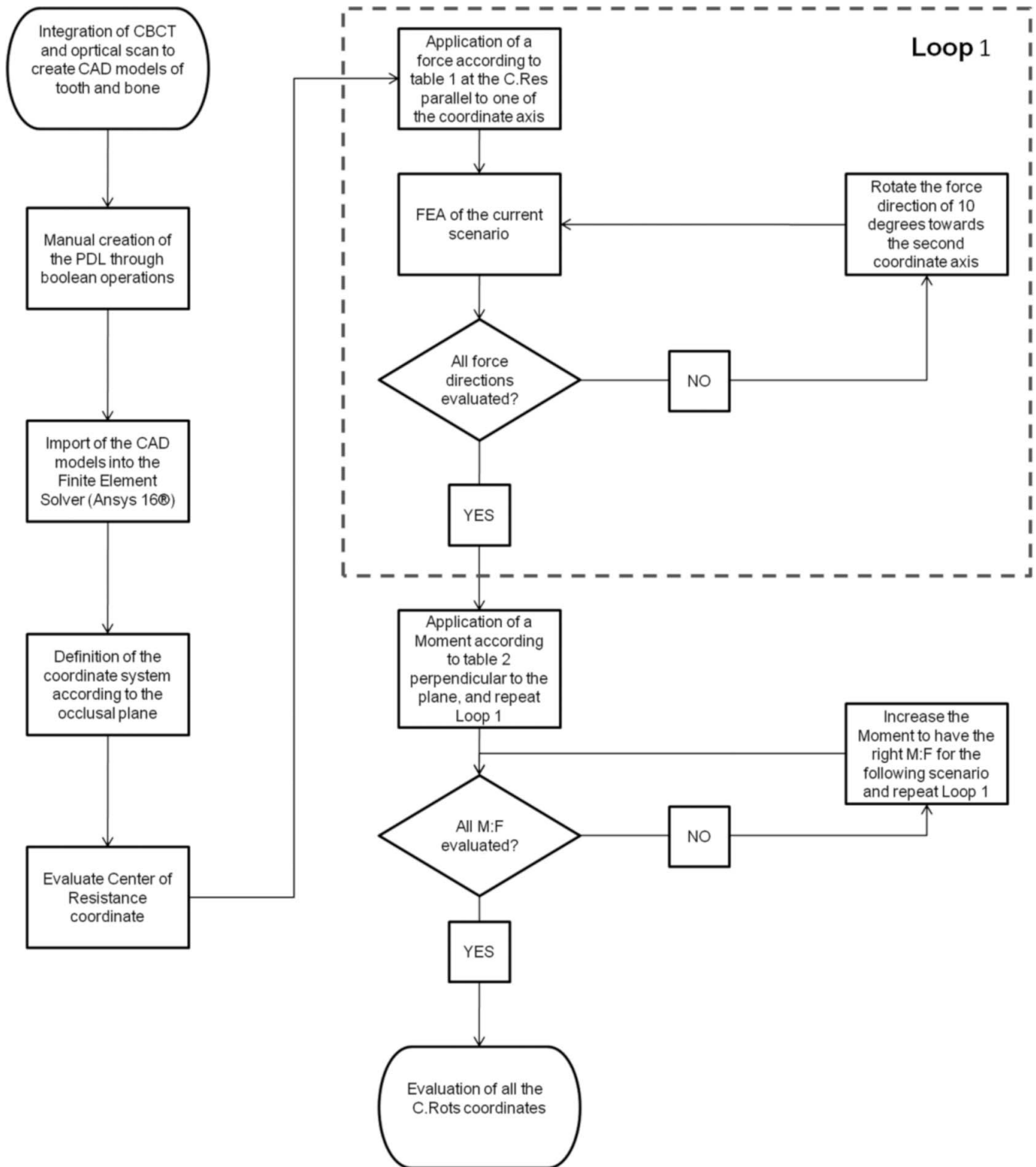


**Figure 2.** Example, plane XY, representation of the incremental directional force system changes (left) and correspondent force systems tipped 10° and 40° with respect to the x-axis for a maxillary first molar (right). Each of the different force and moment combinations at the  $C_{RES}$  was equivalent to one of the 17 single forces spaced 2 mm or 1 mm from each other, where the central force is applied at the  $C_{RES}$ . The higher resolution force increment (1 mm) was applied in the region M:F = [-4:4]. To vary directions, the force was constant, but its direction for each position was changed in the spatial plane of interest in 10° increments, resulting in 10 different simulations for each M:F value at the  $C_{RES}$ .



Downloaded from <http://meridian.allenpress.com/angle-orthodontist/article-pdf/90/6/811/12631036/0003-3219-90-6-811.pdf> by guest on 28 November 2020

**Figure 3.** Experiment workflow.

applied to the tooth to calculate its k values. Then, the  $C_{RES}$  coordinates and k values were derived using the covariates obtained by the regression models, and the two FEA data sets were then compared.

**RESULTS**

The statistical analysis demonstrated that the  $C_{RES}$  coordinates can be calculated using the set of covariates shown in Table 4 at a significance level of

**Table 4.**  $C_{RES}$  Coefficients for Each Tooth<sup>a</sup>

Coordinate	Arch	Coefficient	Unstandardized Coefficients		95.0% Confidence Interval for B		
			B	Significance	Lower Bound	Upper Bound	
X	Mandibular	(Constant)	0.023	.983	-2.273	2.318	
		MD (mm)	0.186	.214	-0.125	0.496	
		LB (mm)	-0.090	.730	-0.647	0.468	
	Maxillary	(Constant)	0.733	.558	-1.936	3.403	
		MD (mm)	-0.285	.177	-0.720	0.150	
		LB (mm)	0.210	.306	-0.221	0.642	
Y	Mandibular	(Constant)	1.493	.007	0.489	2.497	
		LB (mm)	-0.258	.002	-0.404	-0.111	
	Maxillary	(Constant)	-0.218	.813	-2.180	1.744	
		LB (mm)	0.014	.896	-0.222	0.250	
	Average Z	Mandibular	(Constant)	0.112	.886	-1.569	1.793
			$R_{YZ}$ (mm)	0.793	.005	0.301	1.286
$R_{ZX}$ (mm)			-1.164	.000	-1.625	-0.703	
Maxillary		(Constant)	1.529	.194	-0.901	3.959	
		$R_{YZ}$ (mm)	0.122	.471	-0.238	0.482	
		$R_{ZX}$ (mm)	-0.618	.002	-0.965	-0.271	

<sup>a</sup> LB indicates linguobuccal dimension at the cemento-enamel junction (CEJ); MD, mesiodistal dimension at the CEJ;  $R_{YZ}$ , root length on the plane YZ;  $R_{ZX}$ , root length on the plane ZX. The predictors used to calculate the  $C_{RES}$  are the unstandardized coefficients.

.05). Different equations were found for each spatial coordinate stratified by maxillary and mandibular teeth. The statistical analysis showed that  $k$  can be predicted by using the root dimensions, the force direction, and the spatial plane, as hypothesized.

The results also might imply that a different set of covariates should be considered for each plane, with additional distinction placed upon the tooth morphology.

The width of the 95% confidence intervals for the  $k$  covariates varied considerably and lack the power to be considered as reliable for several of the coefficients.

Each hyperbolic equation was characterized by the constant of proportionality ( $k$ ), which depended on the plane, the force's direction, and the tooth (Table 5), as classically defined by Burstone<sup>5</sup> and generalized in 3D by Savignano and Viecilli.<sup>10</sup>

Figure 4 shows the  $k$  shapes for the first patient and indicated that  $k$  increased greatly when the force direction became parallel to the tooth long axis ( $z$ -axis). In addition, the  $k$  values were larger on the YZ and ZX planes than on the XY plane, which contained the mesiodistal and buccolingual dimensions of the teeth. These findings generalized for every tooth confirmed the results obtained by a previous study on a first maxillary premolar.<sup>10</sup>

After calculating the  $C_{ROT}$  location for all of the different load systems, it was confirmed that the M:F and the  $D_{(C_{RES}-C_{ROT})}$  had an hyperbolic relationship in every tooth, characterized by the parameter  $k$ , which changed for each tooth and each force system.

The  $k$  variability was different among different teeth and among different planes for the same tooth. The analysis of the  $k$  values on the different planes showed

that they depended not only on the force direction but also on the moment direction.

$K$  could be predicted with the set of covariates shown in Table 5 at a statistically significant level ( $P < .05$ ). It was possible to retrieve different equations for each tooth and planes, and hence, it was possible to estimate  $k$  for every tooth in any direction in this manner.

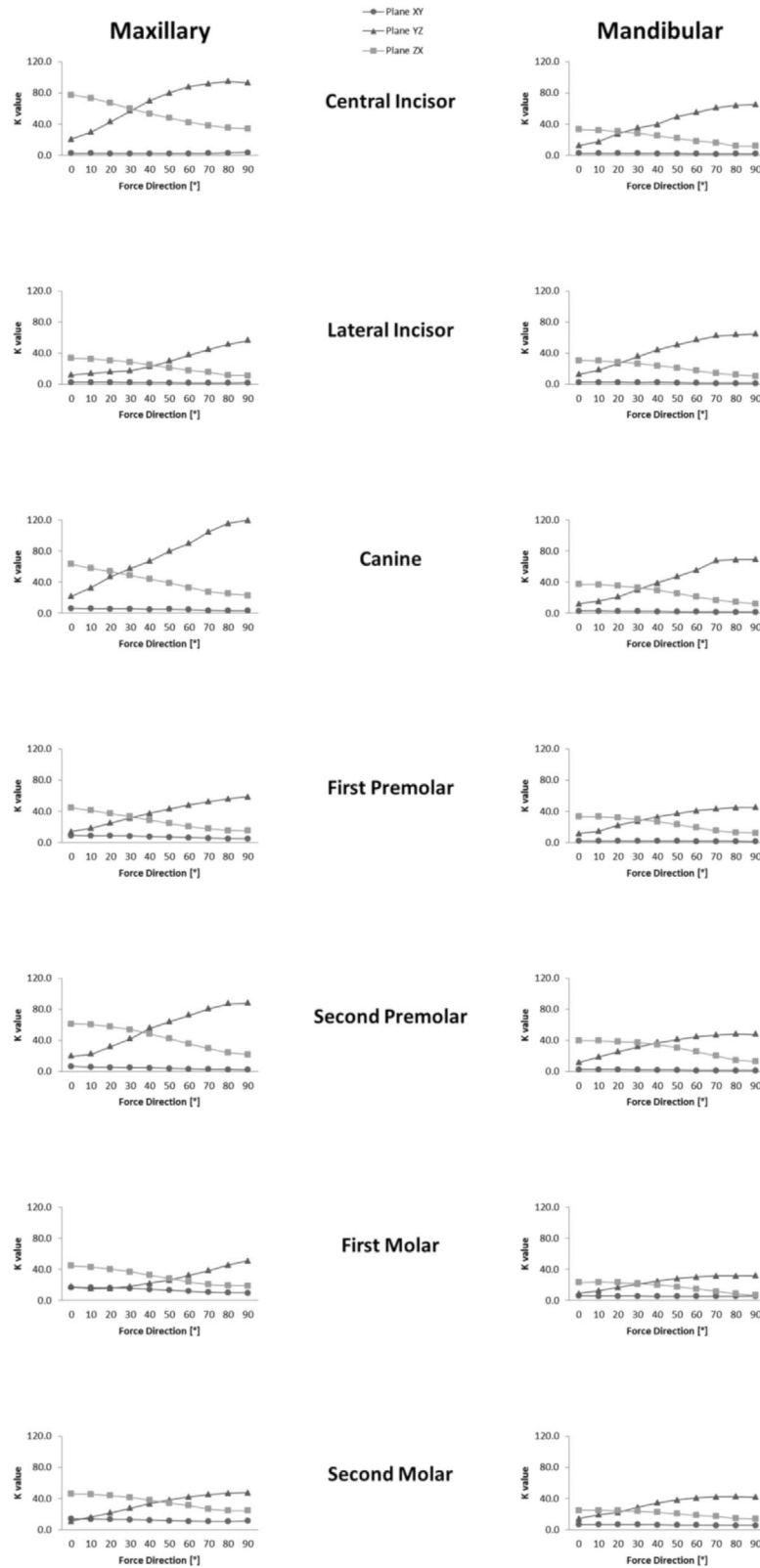
A random mandibular central incisor was chosen to show the covariates' efficacy.

Table 6 and Figure 5 show the  $k$  data sets obtained on a random mandibular central incisor through FEA and morphological covariates, respectively.

## DISCUSSION

The relationship between M:F and initial tooth movement was previously investigated by other researchers. The limitation of the previous studies<sup>2,5-7,9,16</sup> was that they did not relate the effect of M:F variations with tooth morphology, thus making it a necessary requirement to run additional and advanced computations to obtain tooth response curves. Only one study showed in two different teeth that they had a different orthodontic response to M:F variations.<sup>7</sup> This study, although providing more comprehensive 3D data, also had a limitation, which was the simplified linear PDL model. This choice was justified because the loads modeled were below the strain threshold where the PDL starts to stiffen. In a PDL nonlinear model, the responses and  $k$  values would likely be different for different loads.<sup>15</sup>

The statistical analysis provided a set of covariates to calculate the  $C_{RES}$  coordinates and an approximate



**Figure 4.** Graphical representation of k vs force direction for each tooth on the different planes for patient 1. The force direction is reported on the horizontal axis and the k value on the vertical axis. The direction is referred as the angle between the force and the first coordinate axis for each plane.

**Table 5.** k Coefficients for Each Tooth<sup>a</sup>

Tooth	Plane	Model	Unstandardized Coefficients		95.0% Confidence Interval for B		
			B	Significance	Lower Bound	Upper Bound	
LR1	XY	(Constant)	-2.925	.000	-3.799	-2.051	
		R <sub>VZ</sub> , mm	0.436	.000	0.366	0.506	
		Angle, °	-0.012	.000	-0.014	-0.010	
	YZ	(Constant)	70.928	.002	32.288	109.568	
		Angle, °	0.642	.000	0.547	0.738	
		R <sub>AVG</sub> , mm	-4.224	.010	-7.226	-1.221	
	ZX	(Constant)	94.826	.000	67.200	122.452	
		R <sub>VZ</sub> , mm	-4.309	.001	-6.511	-2.107	
		Angle, °	-0.353	.000	-0.418	-0.288	
LR2	XY	(Constant)	-2.726	.009	-4.619	-0.834	
		Angle, °	-0.018	.000	-0.022	-0.013	
		R <sub>ZX</sub> , mm	0.453	.000	0.294	0.613	
	YZ	(Constant)	11.913	.003	5.196	18.629	
		Angle, °	0.641	.000	0.524	0.758	
		(Constant)	1.727	.827	-15.892	19.346	
	ZX	Angle, °	-0.269	.000	-0.303	-0.236	
		R <sub>ZX</sub> , mm	2.457	.004	1.056	3.858	
		(Constant)	-0.172	.651	-1.031	0.688	
LR3	XY	Angle, °	-0.017	.000	-0.019	-0.015	
		R <sub>AVG</sub> , mm	0.240	.000	0.173	0.307	
		(Constant)	9.798	.027	1.454	18.142	
	YZ	Angle, °	0.707	.000	0.525	0.890	
		(Constant)	-82.169	.000	-102.567	-61.771	
		Angle, °	-0.249	.000	-0.286	-0.211	
	ZX	LB, mm	20.289	.000	16.660	23.919	
		(Constant)	-0.084	.775	-0.723	0.554	
		Angle, °	-0.007	.000	-0.009	-0.006	
LR4	XY	R <sub>AVG</sub> , mm	0.193	.000	0.132	0.253	
		(Constant)	-39.448	.029	-74.123	-4.772	
		Angle, °	0.370	.000	0.316	0.423	
	ZX	MD, mm	11.431	.006	3.940	18.922	
		(Constant)	35.153	.000	32.975	37.331	
		Angle, °	-0.257	.000	-0.299	-0.216	
	LR5	XY	(Constant)	-3.723	.002	-5.708	-1.737
			Angle, °	-0.013	.000	-0.019	-0.008
			R <sub>ZX</sub> , mm	0.466	.000	0.321	0.610
YZ		(Constant)	12.244	.000	8.866	15.623	
		Angle, °	0.502	.000	0.434	0.569	
		(Constant)	45.015	.000	41.798	48.232	
ZX		Angle, °	-0.342	.000	-0.406	-0.278	
		(Constant)	-3.485	.014	-6.076	-0.893	
		Angle, °	-0.009	.009	-0.015	-0.003	
LR6	XY	LB, mm	0.988	.000	0.697	1.278	
		(Constant)	-30.629	.004	-48.991	-12.267	
		Angle, °	0.258	.000	0.216	0.300	
	YZ	LB, mm	4.484	.000	2.459	6.509	
		(Constant)	25.996	.000	23.653	28.339	
		Angle, °	-0.210	.000	-0.249	-0.172	
	LR7	XY	(Constant)	-17.535	.000	-19.435	-15.634
			Angle, °	-0.018	.000	-0.023	-0.013
			R <sub>AVG</sub> , mm	2.070	.000	1.902	2.237
YZ		(Constant)	21.989	.000	16.981	26.996	
		Angle, °	0.221	.001	0.117	0.325	
		(Constant)	-5.848	.102	-13.038	1.341	
ZX		R <sub>VZ</sub> , mm	2.834	.000	2.176	3.491	
		Angle, °	-0.147	.000	-0.165	-0.130	



**Table 5.** Continued

Tooth	Plane	Model	Unstandardized Coefficients		95.0% Confidence Interval for B	
			B	Significance	Lower Bound	Upper Bound
UR1	XY	(Constant)	2.404	.000	1.938	2.869
		Angle, °	-0.003	-0.483	-0.012	0.006
	YZ	(Constant)	125.133	.007	45.987	204.280
		Angle, °	0.910	.000	0.754	1.065
		MD, mm	-16.136	.021	-29.082	-3.190
		(Constant)	191.353	.000	156.300	226.407
ZX	Angle, °	-0.505	.000	-0.575	-0.434	
	MD, mm	-18.964	.000	-24.273	-13.656	
	(Constant)	11.043	.000	9.485	12.601	
UR2	XY	Angle, °	-0.012	.000	-0.014	-0.009
		LB, mm	-1.389	.000	-1.646	-1.132
		(Constant)	68.928	.000	37.845	100.012
	YZ	Angle, °	0.490	.000	0.427	0.554
		R <sub>ZX</sub> , mm	-3.791	.002	-5.932	-1.650
		(Constant)	-75.939	.011	-129.368	-22.511
ZX	Angle, °	-0.330	.000	-0.419	-0.241	
	LB, mm	19.624	.001	10.818	28.430	
	(Constant)	-1.744	.027	-3.260	-0.228	
UR3	XY	Angle, °	-0.031	.000	-0.035	-0.027
		LB, mm	0.904	.000	0.717	1.091
		(Constant)	28.181	.000	17.933	38.429
	YZ	Angle, °	1.074	.000	0.885	1.262
		(Constant)	61.654	.000	56.214	67.094
		Angle, °	-0.492	.000	-0.588	-0.396
UR4	XY	(Constant)	28.903	.000	23.958	33.848
		Angle, °	-0.037	.000	-0.048	-0.026
		MD, mm	-4.123	.000	-5.077	-3.170
	YZ	(Constant)	-46.292	.044	-90.973	-1.610
		Angle, °	0.578	.000	0.548	0.608
		LB, mm	6.891	.016	1.685	12.098
ZX	(Constant)	68.744	.000	54.613	82.875	
	Angle, °	-0.321	.000	-0.347	-0.295	
	MD, mm	-5.287	.001	-8.000	-2.574	
UR5	XY	(Constant)	-25.264	.000	-31.561	-18.967
		Angle, °	-0.034	.000	-0.041	-0.027
		R <sub>AVG</sub> , mm	2.182	.000	1.733	2.632
	YZ	(Constant)	20.307	.000	16.277	24.337
		Angle, °	0.810	.000	0.735	0.885
		(Constant)	65.308	.000	62.962	67.654
ZX	Angle, °	-0.467	.000	-0.509	-0.424	
	(Constant)	18.281	.000	16.896	19.666	
	Angle, °	-0.116	.000	-0.140	-0.092	
UR6	YZ	(Constant)	-20.170	.188	-52.002	11.663
		Angle, °	0.464	.000	0.351	0.577
		MD, mm	3.969	.048	0.034	7.905
	ZX	(Constant)	355.044	.001	173.584	536.504
		Angle, °	-0.291	.000	-0.360	-0.221
		LB, mm	-34.624	.003	-55.026	-14.223
UR7	XY	(Constant)	-6.120	.157	-14.954	2.713
		R <sub>YZ</sub> , mm	1.676	.000	0.989	2.364
		Angle, °	-0.072	.000	-0.082	-0.062
	YZ	(Constant)	161.592	.000	99.350	223.833
		Angle, °	0.346	.000	0.268	0.423
		LB, mm	-14.270	.000	-20.236	-8.304
ZX	(Constant)	193.416	.000	155.396	231.436	
	Angle, °	-0.240	.000	-0.279	-0.201	
	R <sub>AVG</sub> , mm	-12.016	.000	-15.036	-8.996	

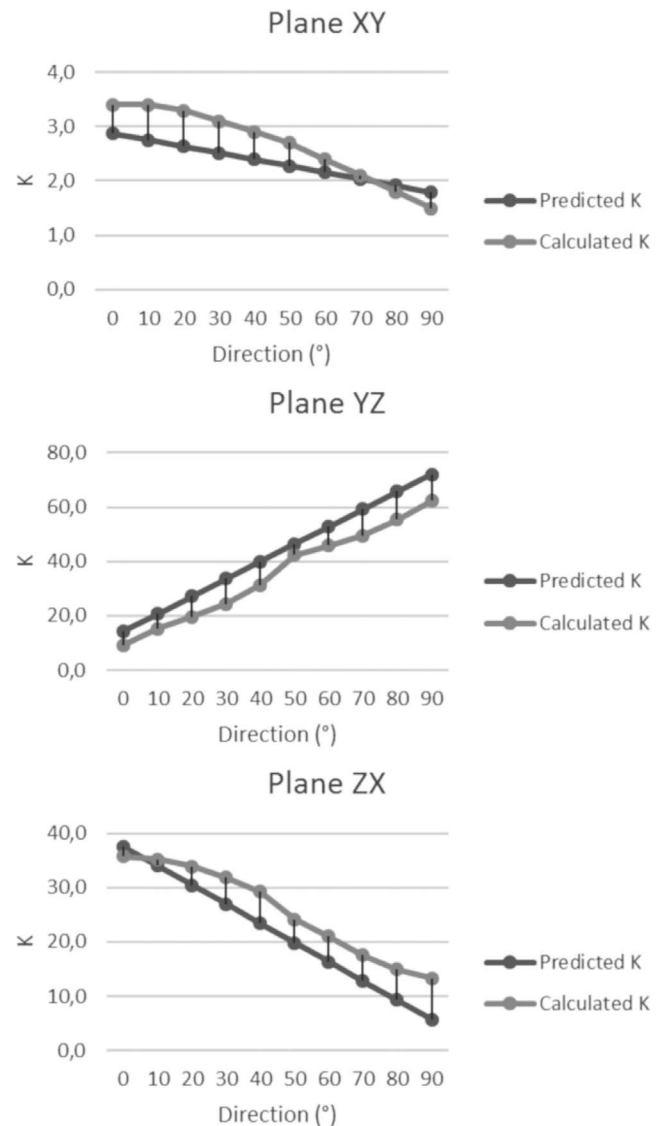
<sup>a</sup> LB indicates linguobuccal dimension at the cementsoenamel junction (CEJ); MD, mesiodistal dimension at the CEJ; R<sub>YZ</sub>, root length on the plane YZ; R<sub>ZX</sub>, root length on the plane ZX; R<sub>AVG</sub>, average between R<sub>YZ</sub> and R<sub>ZX</sub>. The predictors used to calculate k are the unstandardized coefficients.

**Table 6.** Comparison of Predicted and Calculated k Values for a Random Mandibular Central Incisor With MD = 3.3 mm<sup>a</sup>

	Center of Resistance	
	Predicted	Calculated
Loc x, mm	0.9	0.5
Loc y, mm	-0.1	-0.1
Loc z, mm	-5.2	-5.5
	k	
Angle, °	Predicted K	Calculated K
<b>Plane XY</b>		
0	2.9	3.4
10	2.8	3.4
20	2.6	3.3
30	2.5	3.1
40	2.4	2.9
50	2.3	2.7
60	2.2	2.4
70	2.0	2.1
80	1.9	1.8
90	1.8	1.5
<b>Plane YZ</b>		
0	14.3	9.2
10	20.7	15.3
20	27.2	19.5
30	33.6	24.3
40	40.0	31.4
50	46.4	42.3
60	52.8	45.8
70	59.3	49.5
80	65.7	55.4
90	72.1	62.2
<b>Plane ZX</b>		
0	37.5	35.7
10	34.0	35.2
20	30.5	33.9
30	26.9	31.9
40	23.4	29.2
50	19.9	24.1
60	16.3	21.0
70	12.8	17.5
80	9.3	14.9
90	5.7	13.3

<sup>a</sup> LB = 5.2 mm, root YZ = 13.3 mm, and root ZX = 13.5 mm.

k for a random tooth, which described the asymmetric mechanical response of every tooth to an applied load, because of the tooth morphology and force system (Figure 6). The root morphology defined the tooth-specific response to an applied force system. This was likely because the PDL is the most deformable structure and approximately follows the root shape, thus being mathematically related to tooth movement. In addition, the root dimensions weigh differently on the response curves depending on the plane on which the movement occurs and on the number of roots. Both factors define the size of the active contact region between the tooth and PDL (the region where the PDL is in tension or compression).

**Figure 5.** Graphical representation of predicted k vs calculated k for a random mandibular central incisor on each plane.

Orthodontic appliances are usually tested with an electromechanical transducer, capable of measuring in 3D the load system delivered by orthodontic appliances.<sup>17-19</sup> However, the results obtained by transducers cannot be reliably used to predict or approximate the tooth behavior since limited information is available on the different relationship between M:F values and 3D tooth movements for each tooth.

During the evaluation of the appliance's effectiveness, it is recommended to calculate the k for each tooth. Afterward, the errors in the force system delivered to each tooth could be weighted to understand how each error really affected the final expected results, and then a decision can be made as to whether it is an acceptable error or changes are needed in the appliance design.

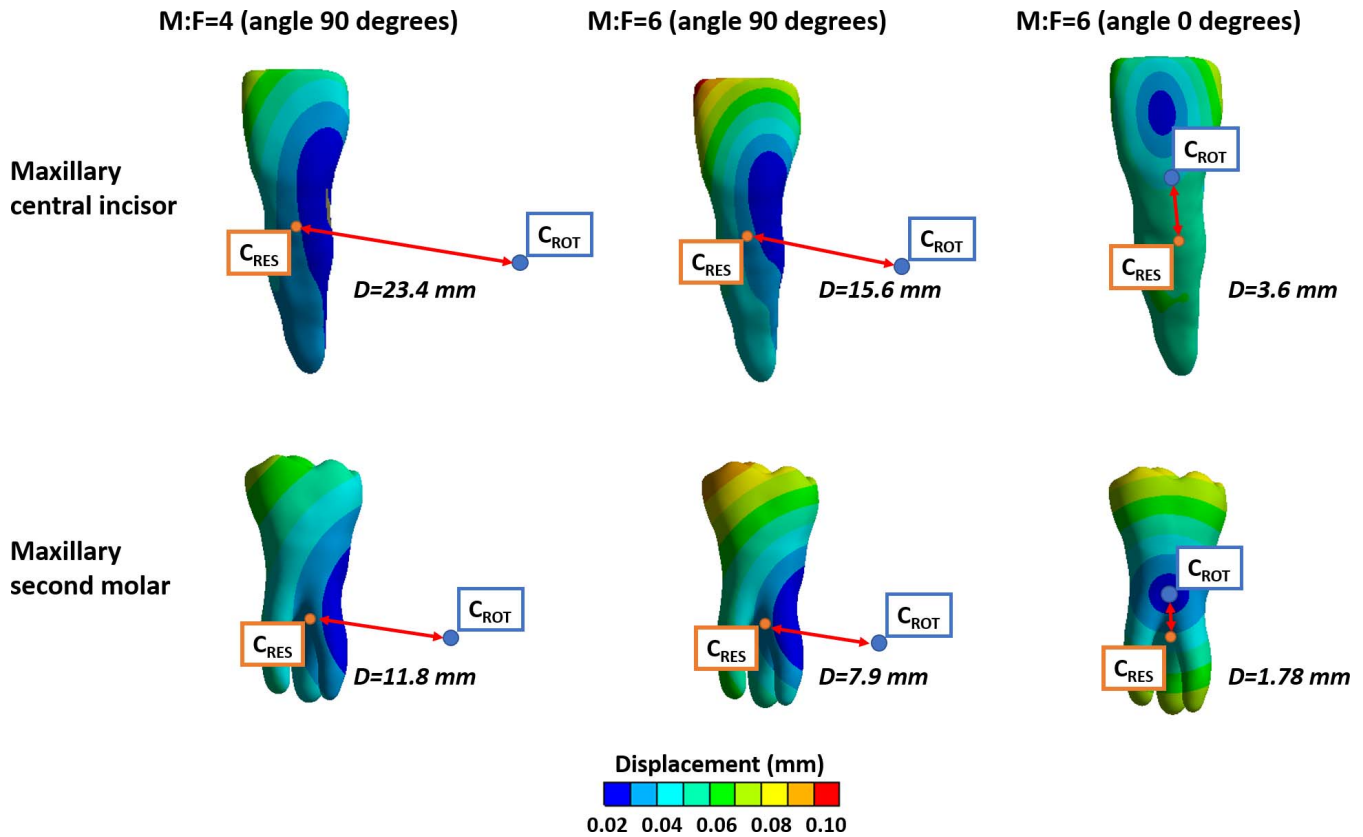


**Figure 6.** The different incremental changes in  $C_{ROT}$  with two M:F values (4 mm and 6 mm) and with two different force directions on the plane YZ for a maxillary central incisor and a maxillary second molar.

It is not practical to calculate  $k$  for each tooth using FEA before every orthodontic treatment. Hence, the set of equations provided by the statistical analysis can be used to calculate an approximate  $k$  knowing the tooth morphology. In particular, it would be necessary to provide a patient’s CBCT to obtain the appropriate variables.

Comparing the results obtained on a random mandibular central incisor through FEA and covariates, respectively, it was noticed that the results were more accurate on the XY (16% average error) than on the ZX plane (26% average error) and on the YZ plane (24% average error). Despite that, the method introduced in the present article showed an overall acceptable accuracy (22% average error), using only the linguobuccal size at the CEJ, mesiodistal size at the CEJ, and root length.

Previous authors have investigated the  $C_{ROT}$  location features. Yang and Tang<sup>12</sup> compared the effect of different M:F on the  $C_{ROT}$  location for a canine tooth, with and without a bracket. Cattaneo et al.<sup>7</sup> tested different M:F values on a premolar and canine and showed how the  $C_{ROT}$  moved closer to the apex with an increase in M:F value.

Provatidis<sup>20</sup> demonstrated that the position of the  $C_{ROT}$  was affected by root dimensions, PDL thickness,

and material properties. On the other hand, the present study aimed at finding a generalized set of predictors for every tooth to estimate  $C_{RES}$  and  $C_{ROT}$  locations, which will allow comparison of the effect of different orthodontic appliances in 3D. The estimation of the expected  $C_{RES}$  and  $C_{ROT}$  coordinates for each scenario could be helpful to easily understand which appliance design provides the best expected movement.

It could be desirable to develop a set of equations that require only tooth crown features and features retrievable by a panoramic radiograph, but it would evidently result in more error. This would allow calculation of the  $k$  data set for a random tooth using a less invasive method based on an optical scan and less radiation.

**CONCLUSIONS**

- The current study showed that it is possible to estimate the approximate  $C_{RES}$  coordinates and the entire tooth movement curve for the initial phase of orthodontic movement, knowing the root dimensions, using separate equations for maxillary and mandibular teeth.

- The results showed that variations of the M:F have a different influence depending on the tooth morphology and the force system features, and the k values are comprised between 1 and 119.4. Therefore, those differences cannot be neglected when estimating tooth movement response curves.
- The geometrical features necessary to calculate k are linguobuccal size at the CEJ, mesiodistal size at the CEJ, root length on the ZX plane, root length on the YZ plane, and average root length. All of these dimensions can be measured using CBCT.
- Using k, it is possible to estimate the distance between the expected  $C_{ROT}$  and the  $C_{ROT}$  obtained by any force system applied to a tooth. This method allows quantification of the potential effectiveness of any orthodontic appliance and selection of the most appropriate one. It is necessary to determine the desired orthodontic movement (expected  $C_{ROT}$ ), the force system delivered by the appliance under examination (actual  $C_{ROT}$ ), and the tooth morphology.
- Further studies should analyze a larger data set and attempt to apply the same method for the whole orthodontic movement, while also accounting for nonlinear PDL behavior.

## ACKNOWLEDGMENTS

The study was supported by the American Association of Orthodontists Foundation. The authors declare no potential conflicts of interest with respect to the authorship and/or publication of this article.

## REFERENCES

1. Croci CS, Caria PHF. Rotation axis of the maxillary molar and maximum tooth movement according to force direction. *Braz J Oral Sci.* 2015;14:130–134.
2. Dathe H, Nagerl H, Kubein-Meesenburg D. A caveat concerning center of resistance. *J Dent Biomech.* 2013;4:1758736013499770.
3. Kondo T, Hotokezaka H, Hamanaka R, et al. Types of tooth movement, bodily or tipping, do not affect the displacement of the tooth's center of resistance but do affect the alveolar bone resorption. *Angle Orthod.* 2017;87(4):563–569.
4. Nyashin Y, Nyashin M, Osipenko M, et al. Centre of resistance and centre of rotation of a tooth: experimental determination, computer simulation and the effect of tissue nonlinearity. *Comput Methods Biomech Biomed Engin.* 2016;19(3):229–239.
5. Burstone CJ. The biomechanics of tooth movement. In: Kraus BS, Riedel BA (eds.): *Vistas in orthodontics*. Lea & Febiger, Philadelphia 1962: 197–213.
6. Burstone CJ, Pryputniewicz RJ. Holographic determination of centers of rotation produced by orthodontic forces. *Am J Orthod.* 1980;77:396–409.
7. Cattaneo PM, Dalstra M, Melsen B. Moment-to-force ratio, center of rotation, and force level: a finite element study predicting their interdependency for simulated orthodontic loading regimens. *Am J Orthod Dentofacial Orthop.* 2008;133:681–689.
8. Smith RJ, Burstone CJ. Mechanics of tooth movement. *Am J Orthod.* 1984;85:294–307.
9. Viecilli RF, Budiman A, Burstone CJ. Axes of resistance for tooth movement: does the center of resistance exist in 3-dimensional space? *Am J Orthod Dentofacial Orthop.* 2013;143:163–172.
10. Savignano R, Viecilli RF, Paoli A, Razionale AV, Barone S. Nonlinear dependency of tooth movement on force system directions. *Am J Orthod Dentofacial Orthop.* 2016;149(6):838–846.
11. Dorow C, Krstin N, Sander F-G. Experiments to determine the material properties of the periodontal ligament. *J Orofac Orthop.* 2002;63:94–104.
12. Yang Y, Tang WC. Analysis of the influences of bracket and force system in different directions on the moment to force ratio by finite element method. *Eurasip J Wirel Comm.* 2018:169.
13. Poppe M, Bourauel C, Jager A. Determination of the elasticity parameters of the human periodontal ligament and the location of the center of resistance of single-rooted teeth a study of autopsy specimens and their conversion into finite element models. *J Orofac Orthop.* 2002;63(5):358–370.
14. Viecilli RF, Burstone CJ. Ideal orthodontic alignment load relationships based on periodontal ligament stress. *Orthod Craniofac Res.* 2015;18(suppl 1):180–186.
15. Kavarizadeh A, Bourauel C, Zhang DL, Gotz W, Jager A. Correlation of stress and strain profiles and the distribution of osteoclastic cells induced by orthodontic loading in rat. *Eur J Oral Sci.* 2004;112(2):140–147.
16. Nagerl H, Burstone CJ, Becker B, Kubeinmessenburg D. Centers of rotation with transverse forces: an experimental-study. *Am J Orthod Dentofacial Orthop.* 1991;99(4):337–345.
17. Hahn W, Dathe H, Fialka-Fricke J, et al. Influence of thermoplastic appliance thickness on the magnitude of force delivered to a maxillary central incisor during tipping. *Am J Orthod Dentofacial Orthop.* 2009;136:12.e11–17.
18. Hahn W, Fialka-Fricke J, Dathe H, et al. Initial forces generated by three types of thermoplastic appliances on an upper central incisor during tipping. *Eur J Orthod.* 2009;31:625–631.
19. Xia Z, Chen J, Jiangc F, Li S, Viecilli RF, Liu SY. Load system of segmental T-loops for canine retraction. *Am J Orthod Dentofacial Orthop.* 2013;144:548–556.
20. Provatidis CG. Numerical estimation of the centres of rotation and resistance in orthodontic tooth movement. *Comput Methods Biomech Biomed Engin.* 1999;2(2):149–156.